Supporting Information for

Pattern dynamics and stochasticity of the brain rhythms

C. Hoffman, J. Cheng, D. Ji, Y. Dabaghian

Y. Dabaghian.
E-mail: Yuri.A.Dabaghian@uth.tmc.edu

This PDF file includes:

Figs. S1 to S5

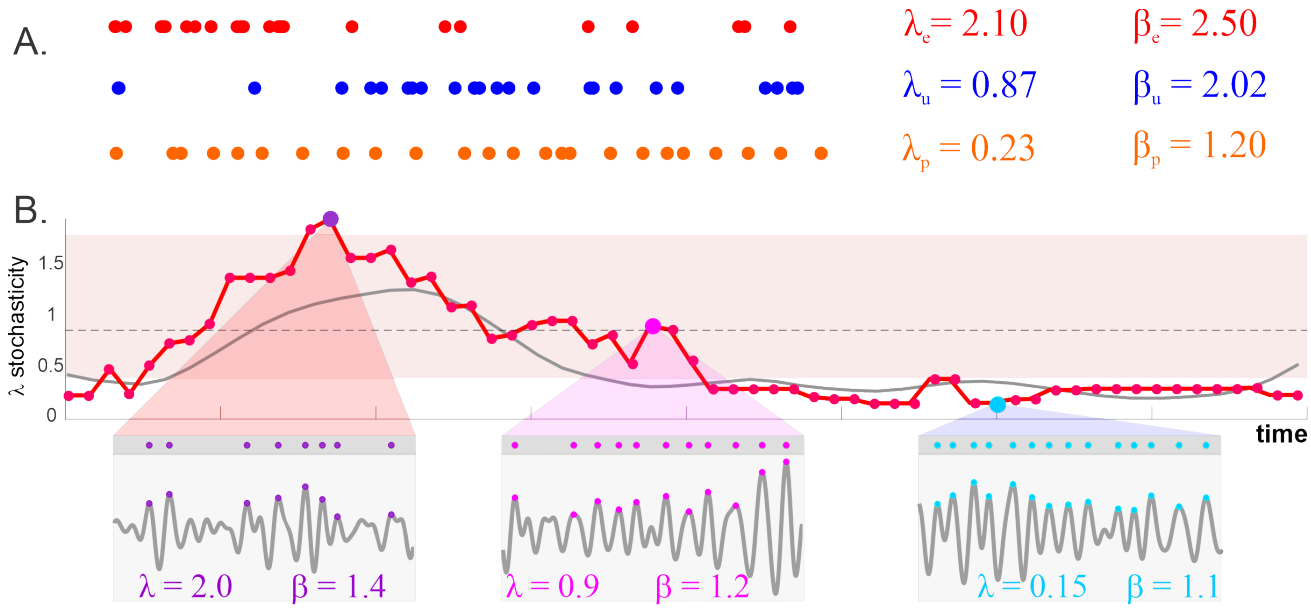

Fig. S1. Examples of patterns with different stochasticity scores. **A**. Examples of randomly generated patterns with high ($\lambda > 1.8$, $\beta > \beta^*$), intermediate ($\lambda \approx \lambda^*$, $\beta \approx \beta^*$) and low ($\lambda < 0.4$, $\beta \approx 1$) stochasticity scores, obtained for $N = 25$ exponentially (top), uniformly (middle), and Poisson-distributed intervals (colors as on Fig. 3). The top pattern with the highest scores is most stochastic, the bottom one, with lowest scores is most orderly. **B**. A segment of the $\lambda(t)$ dependence (dots mark window positions), and three exemplary λ-values: above (lilac dot), within (magenta dot) and below (light blue dot) the domain of stochastic typicality. The higher the λ, the more uneven are the corresponding peak patterns and the underlying waveforms. Gray line in the background represents speed, as on Figs. 4-6.

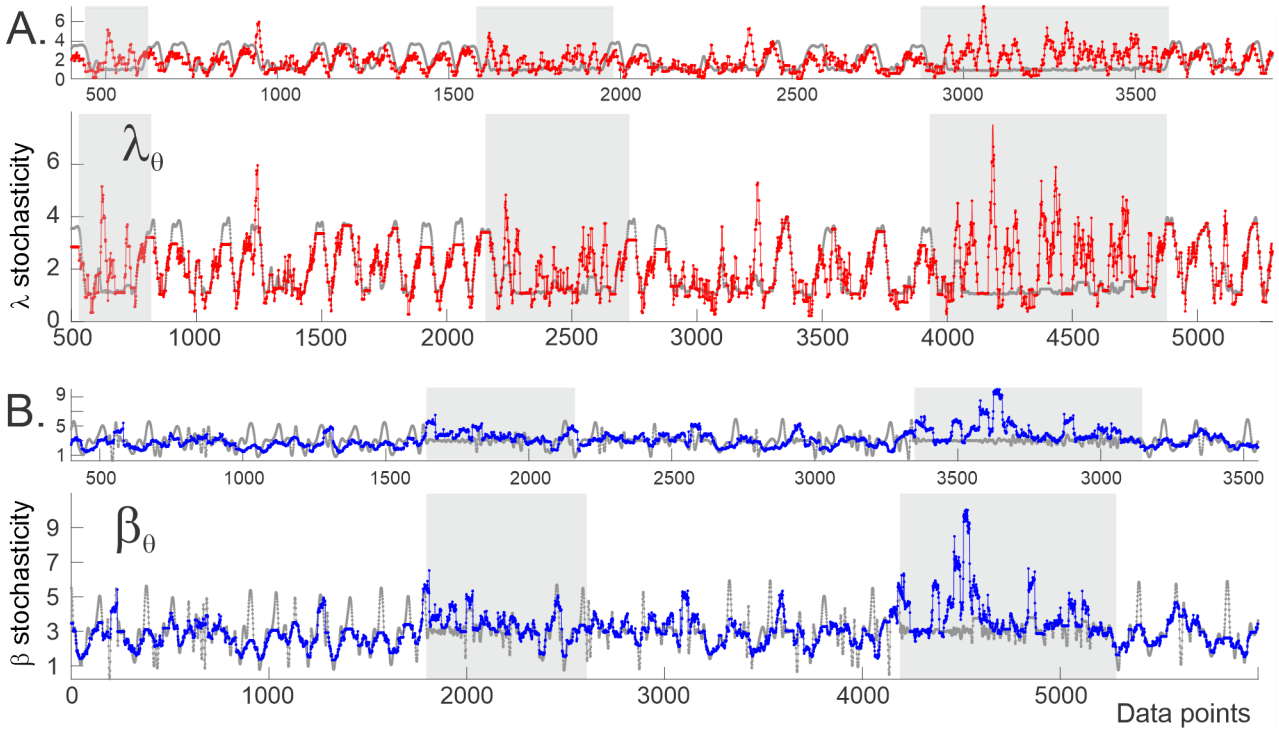

Fig. S2. Matching waves using DTW. **A**. Top panels show the original shapes of the speed ($s(t)$, gray trace) and the θ-wave's Kolmogorov stochasticity score ($\lambda_\theta(t)$, red trace). Bottom panel shows same functions, matched up by a sequences of local DTW-stretches. Clearly, the speed and the λ_θ-stochasticity have the same qualitative shape during active behavior, while during inactive moves (domains marked by light gray stripe) the connection is lost. **B**. Same analyses carried for the mouse's acceleration ($a(t)$, gray trace) and Arnold stochasticity parameter (β_θ, blue trace). The net amount of stretch required to match speed and λ_θ in this case (including the inactivity periods) is 26%, while the net stretch matching β_θ and the acceleration is $\sim 18\%$.

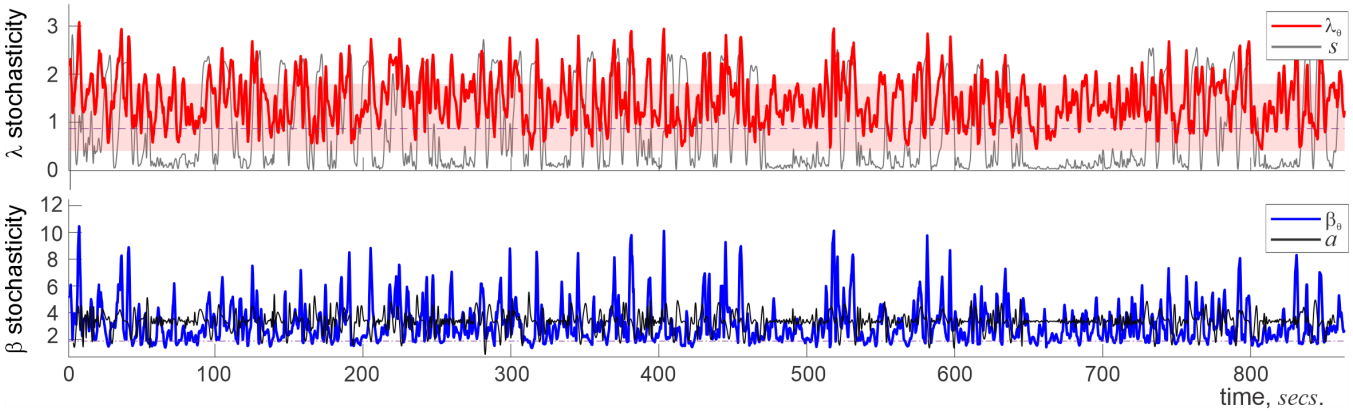

Fig. S3. Aperiodic component of the θ-wave. **A**. The Kolmogorov stochasticity score computed for the patterns of the θ-wave's arhythmicity $\xi_\theta(t)$ (red trace). In contrast with the original θ-wave's stochasticity scores, λ_θ, the λ_ξ-scores are higher, wider-distributed, but show no coupling to the speed, $s(t)$ (gray line), and does not reflect changes in the physiological state. **B**. The corresponding Arnold's stochasticity parameter $\beta_\xi(t)$ (blue trace) is much higher than the original $\beta_\theta(t)$ score, indicating strong cluttering patterns, but without coupling to the mouse's acceleration $a(t)$ (dark gray trace).

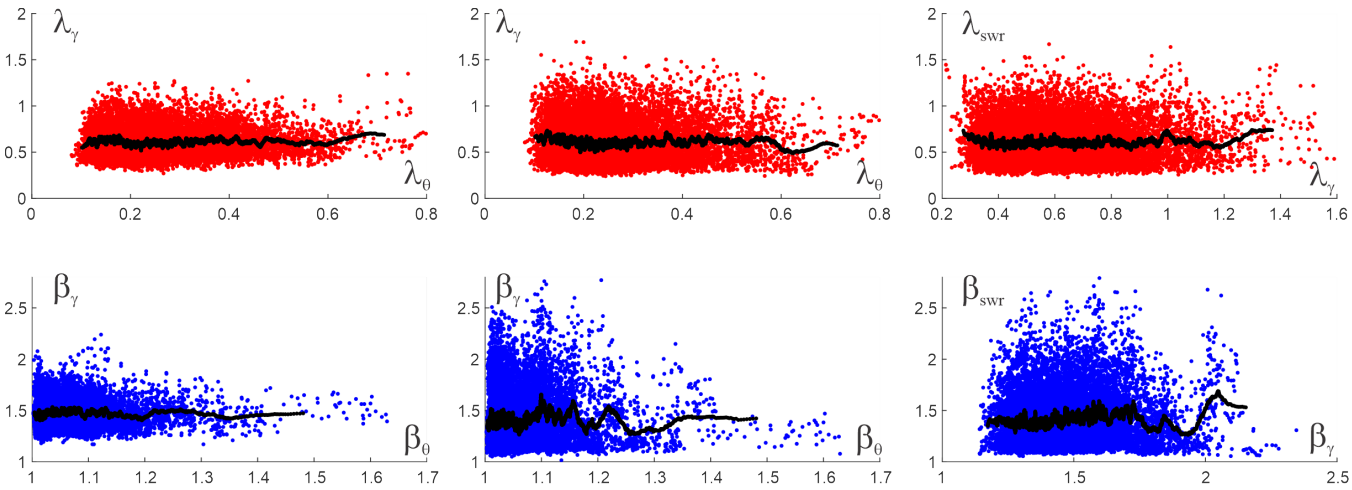

Fig. S4. Coupling between stochasticity parameters of different waves. **A**. The geometric layout of points with coordinates $(\lambda_\theta, \lambda_\gamma)$, $(\lambda_\theta, \lambda_{re})$ and $(\lambda_\gamma, \lambda_{re})$ shows that a given λ-value produced by one wave may pair with any λ-value that another wave is capable of producing, i.e., wave patterns deviate from their respective means largely independently from each other. Correspondingly, the locally averaged scores $\hat{\lambda}$ lay approximately horizontally, at the level of the corresponding means $\langle\lambda_\theta\rangle$, $\langle\lambda_\gamma\rangle$ and $\langle\lambda_{re}\rangle$ (see Fig. 4D, Fig. 5B and Fig. 6B). **B**. The β-scores reveal similar lack of coupling between waves. Changes in locally averaged $\hat{\beta}$-values of one wave not entrain consistent $\hat{\beta}$-changes of another wave. Thus, the (dis)orderliness of one wave does not enforce the (dis)orderliness of the other and the stochasticity dynamics discussed above provide independent characterizations of the LFP waves.

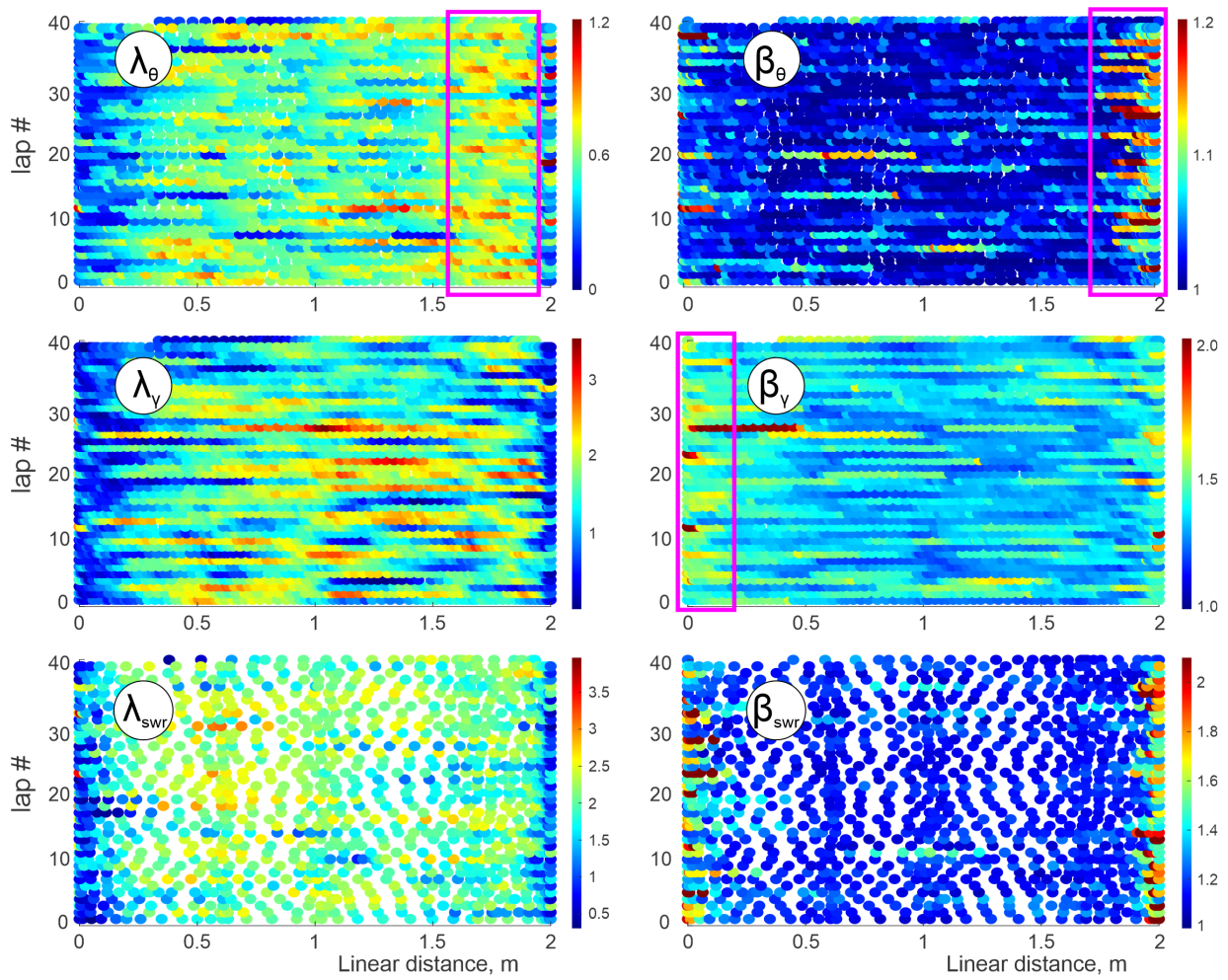

Fig. S5. Linearized stochasticity maps. The spatial distribution of the λ_*-scores along the track (left column) illustrates that the brainwave patterns tend to conform with the expected mean trends at the ends of the runway, i.e., in the vicinity of the food wells. In the middle of the track, the rhythms tend to wobble. Also note that θ-wave exhibits wobbling upon leaving the right food well area (pink square). The β_*-scores (right column) tend to increase at the ends and drop in the middle, i.e., waves are more disordered at the food wells and quasiperiodic during the runs between them.